



Peri-personal space encoding in patients with disorders of consciousness and cognitive-motor dissociation

Jean-Paul Noel^a, Camille Chatelle^{b,c,d}, Serafeim Perdikis^{e,f}, Jane Jöhr^g, Marina Lopes Da Silva^g, Philippe Ryvlin^g, Marzia De Lucia^h, José del R. Millán^e, Karin Diserens^{g,*,1}, Andrea Serino^{i,*,1}

^a Vanderbilt Brain Institute, Vanderbilt University, Nashville, TN, USA

^b Center for Neurotechnology and Neurorecovery, Massachusetts General Hospital, Boston, MA, USA

^c Department of Neurology, Massachusetts General Hospital, Harvard Medical School, Boston, MA, USA

^d Coma Science Group, GIGA Consciousness, University and University Hospital of Liège, Liège, Belgium

^e Center for Neuroprosthetics, School of Engineering, Ecole Polytechnique Federale de Lausanne (EPFL), Geneva, Switzerland

^f Brain-Computer Interfaces and Neural Engineering Laboratory, School of Computer Science and Electronic Engineering, University of Essex, UK

^g Acute Neurorehabilitation Unit, Neurology, Department of and Clinical Neurosciences, University Hospital of Lausanne, Lausanne, Switzerland

^h Laboratoire de Recherche en Neuroimagerie, Department of Clinical Neurosciences, University Hospital of Lausanne, University of Lausanne, Lausanne, Switzerland

ⁱ MySpace Lab, Department of Clinical Neurosciences, University Hospital of Lausanne, University of Lausanne, Lausanne, Switzerland

ARTICLE INFO

Keywords:

Disorders of consciousness
Motor-cognitive dissociation
Electroencephalography
Brain injury
Peri-personal space
Multisensory

ABSTRACT

Behavioral assessments of consciousness based on overt command following cannot differentiate patients with disorders of consciousness (DOC) from those who demonstrate a dissociation between intent/awareness and motor capacity: cognitive motor dissociation (CMD). We argue that delineation of peri-personal space (PPS) – the multisensory-motor space immediately surrounding the body – may differentiate these patients due to its central role in mediating human-environment interactions, and putatively in scaffolding a minimal form of selfhood. In Experiment 1, we determined a normative physiological index of PPS by recording electro-physiological (EEG) responses to tactile, auditory, or audio-tactile stimulation at different distances (5 vs. 75 cm) in healthy volunteers ($N = 19$). Contrasts between paired (AT) and summed (A + T) responses demonstrated multisensory supra-additivity when AT stimuli were presented near, i.e., within the PPS, and highlighted somatosensory-motor sensors as electrodes of interest. In Experiment 2, we recorded EEG in patients behaviorally diagnosed as DOC or putative CMD ($N = 17, 30$ sessions). The PPS-measure developed in Experiment 1 was analyzed in relation with both standard clinical diagnosis (i.e., Coma Recovery Scale; CRS-R) and a measure of neural complexity associated with consciousness. Results demonstrated a significant correlation between the PPS measure and neural complexity, but not with the CRS-R, highlighting the added value of the physiological recordings. Further, multisensory processing in PPS was preserved in putative CMD but not in DOC patients. Together, the findings suggest that indexing PPS allows differentiating between groups of patients whom both show overt motor impairments (DOC and CMD) but putatively distinct levels of awareness or motor intent.

1. Introduction

Detailing the neural and computational mechanisms enabling wakefulness and conscious experience is a central and unanswered question within both systems and clinical neuroscience, with paramount implications for healthcare of patients with disorders of consciousness (DOCs; Bernat, 2006). DOC patients are typically classified either as

comatose, or, if emerging from this state, as within vegetative state/unresponsive wakefulness syndrome (UWS; Laureys et al., 2010) or as within a minimally conscious state (MCS; Giacino et al., 2014). This classification of consciousness-level is routinely performed at the bedside and is based on behavioral tests, such as the Coma Recovery Scale (CRS-R; Giacino et al., 2004). Unfortunately, despite great efforts in improving these observational assessments, they suffer from a number

* Correspondence to: K. Diserens, Acute Neurorehabilitation Unit, Department of Clinical Neurosciences, Neurology, University Hospital Lausanne (CHUV), Rue du Bugnon 46, 1011 Lausanne, Switzerland.

** Correspondence to: A. Serino, MySpace Lab, Department of Clinical Neurosciences, Bâtiment Nestle, University Hospital Lausanne (CHUV), Rue Pierre Decker 5, 1011 Lausanne, Switzerland.

E-mail addresses: karin.diserens@chuv.ch (K. Diserens), andrea.serino@unil.ch (A. Serino).

¹ These authors (listed in alphabetical order) contributed equally and act both as co-senior authors and corresponding authors.

of limitations (Giacino et al., 2009) contributing to a high number of misdiagnoses (Cruse et al., 2012). In particular, due to the fact that bedside responses are highly dependent on motor output, behavioral assessments cannot differentiate between patients with impaired awareness from those with an absent motor outflow (Laureys et al., 2004; Giacino et al., 2009).

In turn, more recently researchers have used neuroimaging techniques (Birbaumer et al., 1999; Owen et al., 2006; Laureys and Schiff, 2012) to demonstrate intentionality in the absence of movement (Owen, 2014; Monti et al., 2010). Further, a novel clinical dimension within DOC diagnosing has been proposed to account for patients - cognitive-motor dissociation (CMD; Schiff, 2015; Edlow et al., 2017; Curley et al., 2018) - with signs of covert command following despite being classified as DOC patients according to the Glasgow Coma Scale (Teasdale and Jennet, 1974) or CRS-R. Likewise, a novel observational clinical tool, the Motor Behavior Tool (MBT; Pignat et al., 2016; Pincherle et al., 2018), supplementary to CRS-R, has been developed and validated to specifically identify subtle motor behaviors that may reflect residual cognition/awareness underestimated by the CRS-R. The MBT, however, still necessitates being cross-validated with neuroimaging techniques; this validation constitutes an aim of the current project.

To provide an electrophysiological assessment of DOC and CMD patients, we leverage a very specific neural network, that encoding Peri-Personal Space (PPS). PPS is the space immediately surrounding the body (Rizzolatti et al., 1997; Graziano and Cooke, 2006; Serino, 2019), which defines where the body can interact with stimuli in the environment (Clery et al., 2015; Serino et al., 2015; Noel et al., 2018a). This space is encoded by multisensory-motor neurons within a frontoparietal network (Graziano et al., 1999, 2000) that respond to tactile stimuli on the body, and to visual and/or auditory stimuli when these are presented within a limited distance from the body. PPS neurons project directly to the motor systems (Matelli and Luppino, 2001; Makin et al., 2009; Serino et al., 2009), and the extent of PPS largely depends on action possibilities, for instance extending during movement (e.g., Noel et al., 2015a; Pfeiffer et al., 2018) or when using a tool to act upon far objects (see Maravita and Iriki, 2004). Further, PPS remaps with the intent of acting upon objects, even in the absence of motor output (Patane et al., 2018). In addition to the connection with the motor system and motor intention, recent experimental findings show that multisensory integration within PPS may scaffold a minimal form of self-awareness (Blanke and Metzinger, 2009; Blanke, 2012; Blanke et al., 2015; Noel et al., 2018b), by supporting body ownership - i.e., the pre-reflexive experience that the body is one's own (Brozzoli et al., 2012) - and self-location (Noel et al., 2015b; Salomon et al., 2017) - i.e. the experience of being at a given, embodied location in space. Thus, the PPS is considered to be an interface for self-environment interactions (Serino et al., 2017; Serino, 2019; Noel et al., 2018b), and therefore may be altered in patients with DOC. Most interestingly, its functioning may differentiate patients evidencing intention, without being able to implement it - i.e., CMD patients - from those who are more severely isolated from the external world given impairments in consciousness - i.e., DOC patients. That is, by contrasting putative CMD and DOC patients' PPS, we may match lack of veridical motor output, while arguably contrasting different level of motor intention and awareness.

2. Materials and methods

2.1. Experimental design and rationale

In order to measure PPS in DOC and putative CMD patients while following a hypothesis driven approach, this study is conducted in two parts. In a first experiment, we determined the electroencephalography (EEG) correlates of audio-tactile PPS surrounding the arm in healthy participants ($N = 19$). We considered PPS to be evidenced when

multisensory integration (i.e., sum of unisensory responses \neq multisensory response) is modulated as a function of observer-stimuli distance (see Avillac et al., 2007; Bernasconi et al., 2018; Noel et al., 2018c). In Experiment 2, we specifically tested the PPS metric developed in Experiment 1 in 17 patients - some of them tested multiple times, leading to a total of 30 observations - along the DOC spectrum. We also distinguished patients with disorders of consciousness without (DOC) and with signs of potential CMD as suggested by the MBT.

Initial data-driven analyses in healthy volunteers (Experiment 1) are conducted on Global Field Power (GFP; akin to spatial standard deviation), reducing 64 degrees of freedom (i.e., electrodes), to a singular one. Once temporal intervals of interest are identified given GFP analyses, the spatial dimension is unfolded and we describe electrodes demonstrating PPS processing in the specific temporal intervals highlighted by GFP analyses. Finally, in patients (Experiment 2), we solely examine the electrodes and temporal interval shown to encode for PPS in Experiment 1; making this second experiment entirely hypotheses-driven and extremely conservative statistically.

2.2. Participants

2.2.1. Experiment 1 - healthy participants

Nineteen healthy participants (9 females, age = 24.4 ± 3.9 years old) took part in this study. All participants were right-handed, self-reported no auditory or somatosensory impairment and had normal or corrected-to-normal vision. Participants provided informed consent to take part in the study, which was approved by the local ethic committee of the canton of Vaud, Switzerland. Participants were remunerated with 20 Swiss Francs for their time.

2.2.2. Experiment 2 - patients

Seventeen patients lying within the DOC spectrum (3 females, age = 47.9 ± 18.5 years old, range = 23–73 years old), as defined by the CRS-R, took part in this study. A total of 30 EEG sessions were completed with these patients (1–5 sessions per patient), for a total of 96 blocks of trials (250 trials/block, 3.2 blocks/session on average, range = 1–7 blocks/session). The number of sessions conducted per patient was dictated by clinical necessities, most notably the availability of the patient for research (as opposed to diagnostic tests or rest) and the length of the patients' stay at the Unit of Acute Neuro-Rehabilitation at the University Hospital of Lausanne (CHUV), Switzerland. Patients were diagnosed by clinical neurologists and neuropsychologists via repeated administration of the Coma Recovery Scale-Revised (CRS-R; Giacino et al., 2004) and the Motor-Behavior Tool (Pignat et al., 2016; see Table 1 for clinical detail and diagnosis according to CRS-R and MBT). The MBT (Pignat et al., 2016; Pincherle et al., 2018) is a clinical motor observational scale aiming at detecting subtle "positive" motor behaviors, e.g., signs of limb, facial, ocular, or oral intention or non-reflexive movements. Residual cognition is considered present - according to this tool - when at least one positive item is rated, resulting in classification of the patient as presenting with possible CMD. It has been shown to possess good inter-rater reliability and ability to identify a subgroup of patients showing residual cognition and/or motor intent - as assessed given eventual recovery (Pignat et al., 2016; Pincherle et al., 2018). Still, no unequivocal measure of CMD is currently available, and the MBT (Pignat et al., 2016; Pincherle et al., 2018) is the behavioral tool within a multimodal toolbox including functional and anatomical neuroimaging (Schiff, 2015; Edlow et al., 2017; Curley et al., 2018) to index putative residual cognition/motor intent. On occasion, when a clinical score did not exist for the day of experimental recordings, a linear interpolation between the most proximal scores was performed; the longest time between clinical scoring and the nearest EEG session was 4 days. Overall, there was no difference in CRS-R between patients classified as putative CMD or DOC ($t = 0.70, p = .48$), highlighting the complementarity (i.e., distinct clinical dimensions) of the CRS-R scale and the observations of motor

Table 1
Demographic information of patients (Experiment 2).

| Subject ID | Days since Injury | CRS-R at assessment | Possible CMD (MBT; 1 = yes, 2 = no) | Blocks | Age | Etiology | CRS-R Classification | Gender; male = 1, female = 2 | Arm; left = 1, right = 2 |
|------------|-------------------|---------------------|-------------------------------------|--------|-----|-----------|----------------------|------------------------------|--------------------------|
| 1 | 24 | 18.4 | 1 | 3 | 73 | Hemorage | MCS | 1 | 2 |
| 2 | 40 | 6 | 1 | 3 | 55 | Hemorage | Coma | 1 | 2 |
| 3 | 30 | 17 | 0 | 3 | 72 | Hemorage | Coma | 2 | 2 |
| 4 | 2370 | 3 | 0 | 3 | 55 | Traumatic | UWS | 1 | 1 |
| 5 | 20 | 14.5 | 1 | 3 | 62 | Traumatic | UWS | 1 | 2 |
| 6 | 24 | 8.14 | 1 | 4 | 25 | Traumatic | UWS | 2 | 2 |
| 6 | 32 | 12.71 | 1 | 3 | 25 | Traumatic | UWS | 2 | 2 |
| 7 | 13 | 6.2 | 0 | 3 | 23 | Traumatic | Coma | 2 | 2 |
| 7 | 13 | 6.2 | 0 | 3 | 23 | Traumatic | Coma | 2 | 2 |
| 8 | 34 | 10 | 1 | 4 | 73 | Traumatic | UWS | 1 | 2 |
| 9 | 26 | 12.63 | 1 | 7 | 53 | Hemorage | Coma | 1 | 2 |
| 10 | 26 | 13 | 0 | 3 | 59 | Traumatic | UWS | 1 | 2 |
| 11 | 9 | 7 | 1 | 4 | 32 | Hemorage | MCS | 2 | 1 |
| 12 | 39 | 23 | 1 | 3 | 58 | Traumatic | MCS | 1 | 1 |
| 11 | 13 | 9 | 1 | 5 | 32 | Hemorage | MCS | 2 | 2 |
| 11 | 34 | 8 | 1 | 4 | 32 | Hemorage | MCS | 2 | 2 |
| 12 | 20 | 17 | 1 | 2 | 58 | Traumatic | MCS | 1 | 1 |
| 12 | 24 | 19 | 1 | 4 | 58 | Traumatic | MCS | 1 | 1 |
| 13 | 29 | 20 | 1 | 2 | 75 | Hemorage | UWS | 1 | 1 |
| 14 | 28 | 3 | 1 | 1 | 59 | Hemorage | UWS | 1 | 2 |
| 14 | 35 | 11 | 1 | 4 | 59 | Hemorage | UWS | 1 | 2 |
| 14 | 38 | 13.6 | 1 | 3 | 59 | Hemorage | UWS | 1 | 2 |
| 11 | 41 | 7 | 1 | 2 | 32 | Hemorage | MCS | 2 | 2 |
| 15 | 16 | 18 | 1 | 2 | 70 | Hemorage | Locked in | 1 | 2 |
| 16 | 6 | 0 | 0 | 3 | 43 | Traumatic | coma | 1 | 2 |
| 11 | 69 | 9 | 1 | 3 | 32 | Hemorage | MCS | 2 | 2 |
| 17 | 31 | 7 | 0 | 3 | 71 | Traumatic | Coma | 1 | 2 |
| 17 | 34 | 11 | 0 | 3 | 71 | Traumatic | Coma | 1 | 2 |
| 17 | 35 | 11 | 0 | 3 | 71 | Traumatic | Coma | 1 | 2 |
| 15 | 33 | 18 | 1 | 3 | 70 | Hemorage | Locked in | 1 | 2 |

behavior by the MBT. Of the included patients, 3 were clinically deemed to be in minimally conscious state (MCS), 1 was in Locked-In with Mesencephalic lesion, 7 suffered from unresponsive wakefulness syndrome (UWS), and 6 were comatose. Given clinical evaluations and administration of the MBT (Pignat et al., 2016), 21 sessions were considered to be conducted with patients classified with putative CMD, while the remaining 9 sessions were conducted in patients likely without CMD (i.e., “true” DOC patients, classified by CRS-R complemented by MBT). Etiologies differed: ischemic stroke or hemorrhage in 9 patients and traumatic brain injury in 8 patients (see Table 1 for detail). Caregivers of every patient provided informed consent to take part in the study, which was approved by the local ethic committee of the canton of Vaud, Switzerland.

2.3. Material and apparatus

2.3.1. Experiment 1 – healthy participants

Auditory stimulation was administered at different distances while tactile stimuli were applied on the participants' arm. The auditory stimuli consisted of 50 ms of white noise administered via loudspeakers (Z120 Portable Speakers, Logitech, Lausanne, Switzerland) placed 5 cm (65.2 dB Sound Pressure Level (SPL)) and 75 cm (64.1 dB SPL) from the participant's extended arm in the depth dimension (see Fig. 1). Tactile stimuli were equally 50 ms (pulses at 35 Hz) in duration and administered via functional electrical stimulation (FES; MEDEL Medical Electronics, MOTIONSTIM 8, Innsbruck, Austria) and two electrodes (positive and negative, Flextrode Plus) placed on the extensor *digitorum communis* (i.e., dorsal part of the arm approaching the elbow) at 70% of each participant's motor threshold, which was determined immediately prior to initializing the experimental procedure. Somatosensory stimulation ranged between 5 mA and 11 mA. In addition to the two electrodes placed on the participant's right arm for delivery of tactile stimulation, an additional contact was placed on their right shoulder (depicted in Fig. 1 between electrodes solely for illustration purposes).

This last electrode was connected to earth ground in order to nullify putative electrical artifacts pertaining to the FES stimulation. In the case of multisensory trials, auditory and tactile stimuli were administered synchronously. A host of previous studies using a similar paradigm demonstrate facilitated tactile reaction times (e.g., Noel et al., 2018d, 2018f) or increased corticospinal excitability and amplitude of motor evoked potentials (MEP; Makin et al., 2009; Serino et al., 2009, 2011) induced by transcranial magnetic stimulation when auditory or visual stimuli are presented in PPS. In turn, it is possible that this paradigm elicited covert motor intent, which arguably leads to the mentioned alteration in MEP. However, this possibility is speculative and the explicit purpose of this paradigm, as in Canzoneri et al., 2012, was to index the PPS – an encoding of space thought to reflect the general (and not necessary current) possibility for action.

2.3.2. Experiment 2 – patients

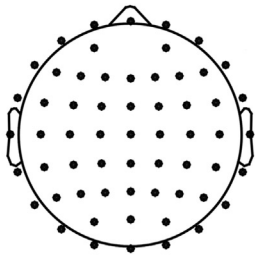
Materials and apparatus were identical as described for Experiment 1 with the exception that for 3 patients, FES was given on the left arm, as opposed to right arm in the rest of patients and healthy participants, due to either configuration constraints or traumatic brain injury impeding EEG on the left brain. For these patients, EEG recordings were left right symmetrically flipped.

2.4. Procedure

2.4.1. Experiment 1 – healthy participants

Participants sat at a table in a light and sound-controlled environment. Electrodes were placed on their arm, and their FES motor threshold was determined. Accordingly, the intensity of tactile stimulation was set (70% of motor threshold), and participants were asked to close their eyes and simply relax. Three blocks of audio-tactile stimulation were conducted. Each block consisted of 250 trials; 50 unisensory tactile, 50 unisensory audio near, 50 unisensory audio far, 50 audio-tactile near, and 50 audio-tactile far. The order of these trials was fully

TD participants – 64 electrodes



DOC/CMD patients – 16 electrodes

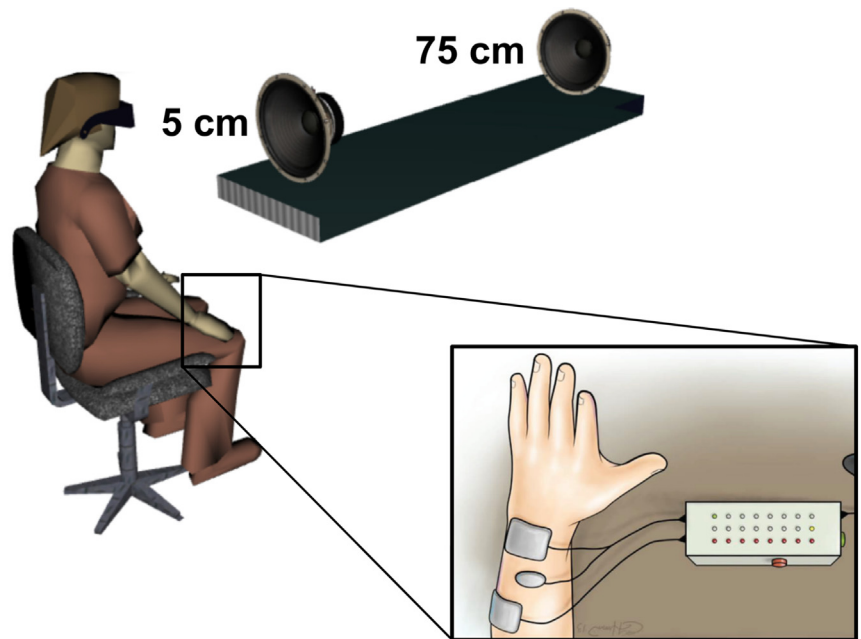
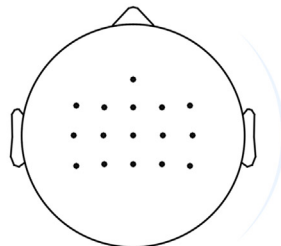


Fig. 1. Methods. Healthy participants (Experiment 1) and patients with disorders of consciousness (CMD patients; Experiment 2) were exposed to tactile (FES stimulation), auditory (white noise), and audio-tactile stimulation while EEG was recorded. A full montage with 64 electrodes was used in healthy participants (top left), while 16 electrodes (bottom left) centered on somatosensory and parietal regions were recorded due to clinical limitations and results from Experiment 1. Auditory stimulation could be administered either close (~5 cm) to the participant's arm (location of tactile stimulation), or far from the arm (~75 cm). In turn, there were a total of 5 conditions; tactile alone, auditory near alone, auditory far alone, audio-tactile near, audio-tactile far.

randomized within a block and inter-trial interval consisted of 1.5–2 s (uniform distribution). Each block of trials had a duration of 10 min. Between blocks participants were given a short break and allowed to open their eyes.

2.4.2. Experiment 2 – patients

Procedures were as in Experiment 1 with the following exceptions. First, patients laid in a supine position (approximately 130°) while testing occurred. Secondly, due to clinical demands a variable number of blocks were recorded in patients, averaging 3.2 blocks per session and ranging from 1 to 7 blocks per session.

2.5. EEG acquisition and preprocessing

2.5.1. Experiment 1 – healthy participants

Continuous EEG was collected via a 64-channel EEG system (g.tec medical engineering, GmbH, Graz, Austria) with a sampling rate of 512 Hz (g.Hlamp, g.tec medical engineering, GmbH, Graz, Austria) and referenced to the average of electrical activity at the left and right earlobes. Data were acquired with in-house EEG acquisition software (eegdev; <http://cnbi.epfl.ch/software/eegdev.html>) developed by the CNBI lab at EPFL and further pre-processed using MATLAB and EEGLAB (Delorme and Makeig, 2004). In pre-processing, data were notch filtered at 50 Hz and bandpass filtered from 0.1 Hz to 40 Hz using a 4th order bi-directional zero-phase infinite impulse response (IIR) filter (hardware bandpass filter is 6th order Butterworth filter between 0.01 and 100 Hz). Epochs from 100 ms before to 500 ms after stimuli onset were extracted for each condition separately. Artifact contaminated trials and bad channels were identified and removed through a combination of automated rejection of trials in which any channel exceeded $\pm 200 \mu\text{V}$ and rigorous visual inspection. A mean of 139.1 (S.E.M = 2.5) trials per conditions were retained (92.7%), while 0.7% (S.E.M = 0.43%) of channels were removed per participant. Bad

channels were reconstructed using spherical spline interpolation (Perrin et al., 1987). Lastly, epochs were baseline corrected to the 100 ms pre stimulus onset. No re-referencing (e.g., to the average) was done, as patients did not count with a full montage (i.e., electrodes covering the entire surface of the skull, but instead for clinical-ease reasons patients counted only with sensors placed above sensorimotor and parietal regions; see Fig. 1). As the estimation of average reference, Global Field Power, and topographical analyses are best approximated when the electrode montage covers uniformly the whole scalp (Lehman & Skrandies, 1980; Murray et al., 2008; Koenig and Melie-Garcia, 2010), the average re-referencing was inappropriate in Experiment 2, and in turn not applied in Experiment 1.

2.5.2. Experiment 2 – patients

Acquisition and pre-processing was as for Experiment 1, with the following exceptions. Continuous EEG was collected via a 16-channel EEG system (g.USBamp and g.Nutilus, g.tec medical engineering, GmbH, Graz, Austria) with a sampling rate of 500/512 Hz and referenced to the right earlobe. Sensors were positioned to cover motor and somatosensory areas (Fz, FC1-FC4, FCz, C1-C4, CZ, CP1-CP4, CPz). A mean of 41.1 (S.E.M = 1.2) trials per condition/block were retained (82.2%). No channels were removed in patients.

2.6. Analyses

2.6.1. Experiment 1 – Global Field Power

The global electric field strength was quantified using Global Field Power (GFP; Lehman & Skrandies, 1980). This measure is equivalent to the spatial standard deviation of the trial-averaged voltage values across the entire electrode montage at a given time point, and represents a reference- and topographic-independent measure of evoked potential magnitude (Murray et al., 2008; Koenig and Melie-Garcia, 2010). This measure is used here to index the presence (or absence) of

evoked potentials during tactile, auditory near, auditory far, audio-tactile near, and audio-tactile far trials. Further, it is used as a data-reduction technique by summarizing 64 distinct time-series (i.e., electrodes) into a singular one. In a first pass, we calculated average GFPs for each subject, as well as for the population of participants as a whole (i.e., grand average) and for every condition. Time-resolved *t*-tests against zero were performed at each time-point from 100 ms pre-stimuli presentation to 500 post-stimuli onset in order to determine periods of significant evoked potentials.

After demonstrating the presence of evoked potentials relative to baseline, to ascertain true multisensory integration, we contrasted the GFP evoked by the audiovisual condition (near and far), to the sum of the unisensory responses (e.g., Cappe et al., 2010; Noel et al., 2018e). The subject average response (at the voltage level and for all 64 electrodes separately) to near and far auditory presentation were summed to the subject's response to tactile stimulation alone, and GFP was computed again. A time-resolved ANOVA was computed at each time-point in order to determine main effects of distance (near vs. far) and sensory stimulation type (paired = AT vs. sum = A + T). Further, after baseline correction, we assessed the interaction between distance and sensory stimulation. This latter effect is of central interest, as it would reveal a PPS effect; namely, a multisensory effect that is space dependent (see Bernasconi et al., 2018 for a similar rationale).

2.6.2. Experiment 1 – event-related potentials

ERPs were obtained by time domain-averaging trials binned for each condition and for each electrode separately at the single-subject level and then averaging across subjects. Given our interest in indexing PPS – a multisensory spatial phenomenon – in an initial pass we focused on the AT near and far conditions. Further, given the GFP results demonstrating multisensory integration within two restricted time-periods (see below) - time period t1 (191ms to 238 ms post-stimuli onset) and t2 (332–384 ms post-stimuli onset) - we initially focused ERP analyses within these timeframes. This analysis revealed a number of electrodes demonstrating a spatial modulation of multisensory responses, and hence likely driving the GFP results. Nonetheless, solely 2 of these electrodes – C4 and CP4 – were present in both time-periods (t1 and t2) and were recorded in DOC patients. Thus, to derive a normative model of what ought to be expected as a PPS correlate in the named electrodes, we averaged these electrodes together and examine the time-course of auditory, tactile, and audio-tactile evoked responses. Here the analysis followed the rationale explained above for the GFP results (i.e., EEG index of PPS = [(A_{near} + T) - AT_{near}] - [(A_{far} + T) - AT_{far}] ≠ 0, see Bernasconi et al., 2018 for a similar approach). Namely, we examined the presence of evoked potentials, then constructed summed responses and contrasted the effect of spatial location (personal vs. extra-personal space) as a function of whether a true multisensory stimuli had been presented or not (i.e., summed A + T vs. paired AT responses as a function of auditory distance). Further, for completeness we report the difference in evoked activity to auditory alone and audio-tactile stimulation as a function of distance. As for the GFP analyses, in order to account for the inherent multiple comparisons and auto-correlation problem in EEG, we set $\alpha < 0.05$ and a temporal criterion of at least 5 consecutive time points (Guthrie and Buchwald, 1991).

2.6.3. Experiment 1 - topographic analyses

GFP and ERP analyses index differences in neural strength, amplitude, and/or latency, but do not take into account the relative spatial distribution of voltages across the scalp as an interesting dependent variable. Hence, here for completeness, and taking advantage of counting with a full-montage of electrodes in healthy participants, we performed topographical analyses. Changes in EEG topography forcibly follow from changes in the configuration of the underlying active electric dipoles (Lehmann, 1987; although the contrary is not necessarily true), and thus, the performed topographical analyses index

when experimental conditions activated distinct sets of brain networks. To test the topography of evoked potentials as a function of sensory stimulation (paired vs. sum) and distance (near vs. far), we used a Global Dissimilarity measure (DISS; Lehmann and Skrandies, 1980). DISS is equivalent to the root-square-mean difference between the potentials measured at each electrode for different conditions, normalized by the instantaneous GFP (L2-norm, in this case). Statistically, the DISS value at each time point was compared to an empirical distribution derived from permuting the condition label of the data from each participant. This analysis is based on a non-parametric randomization procedure (5000 randomizations per time point) and is implemented in the RAGU software (Koenig et al., 2011). Significance threshold was set here to $\alpha < 0.05$, and a time-resolved 2 (sensory stimulation; paired vs. sum) x 2 (distance; near vs. far) topographic ANOVA (TANOVA) on DISS values was performed to identify statistical differences between neural generator configurations for the distinct sensory stimulations as a function of distance. Further, as these analyses revealed a significant sensory stimulation type by distance interaction (in addition to main effects, see below), we moreover segmented these topographies into distinct microstates via topographic cluster analysis based on a hierarchical clustering algorithm (Murray et al., 2008). This clustering identifies stable electric topographies (i.e., “microstates” or “maps”). The optimal number of maps (i.e. the minimal number of microstates accounting for a large portion of the datasets variance) was determined using a modified Krzanowski-Lai criterion (see Murray et al., 2008). Microstates identified in the grand average response (AT_{near}, AT_{far}, A_{near}+T, A_{far}+T) were then back fitted in a procedure wherein each time point for every single-subject condition-specific average evoked response is labeled according to the template map with which it best correlates (Murray et al., 2008). These back-fitted maps can then be statistically contrasted for the duration and interval over which they are present as a function of sensory stimulation and distance condition.

2.6.4. Experiment 2 - event-related potentials

We a priori selected electrodes C4 and CP4 as sensors of interest, as well as t1 (191ms to 238 ms post-stimuli onset) and t2 (332–384 ms post-stimuli onset) as time-periods of interest, given findings from Experiment 1. Within these spatio-temporal constraints, we first measured the strength of the PPS effect within DOC and putative CMD patients and then we compared it with healthy participants (Experiment 1), as well as between putative CMD and DOC patients, via a mixed-model ANOVA (contrast between multisensory pair and summed A + T conditions is a within-subjects variable, while contrast across patients/groups is a between-subjects factor). We equally extracted auditory and tactile evoked potentials in patients (regardless of distance and across their entire montage) given peak amplitudes of GFP in healthy participants. This data is not presented here in detail for brevity, but importantly demonstrated no difference in auditory ($p = .91$) or tactile ($p = .83$) evoked potentials across putative CMD and non-CMD patients. Lastly, given the vast heterogeneity in neural responses in patients due to the distinct ages, causes of disorder, and DOC and putative CMD diagnoses within this group, we examined the relationship between diagnosis of consciousness (both via the clinical scale and a measure of neural complexity associated with consciousness, see below) and the PPS metric (see Results). Of note, the PPS metric and diagnosis of consciousness are performed for each session separately (a total of 30 sessions) and not averaged across sessions and within patients (a total of 17 patients), as DOC diagnosis and CRS-R scores may change across sessions, as does precise EEG montage placement.

2.6.5. Experiments 1 & 2 - EEG complexity

Recent studies have suggested that EEG signal complexity – particularly that evoked by transcranial magnetic stimulation (Casali et al., 2013) – may be a reliable index of consciousness level, being sensitive

to changes induced by psychedelic drugs (Schartner et al., 2017a), non-REM sleep (Andrillon et al., 2016; Schartner et al., 2017b), anesthesia (Zhang et al., 2001; Sarasso et al., 2015; Schartner et al., 2015), or in disorders of consciousness (Casali et al., 2013). Hence, here we applied the Lempel-Ziv complexity (LZc; Lempel and Ziv, 1976) algorithm as a proxy EEG-based metric of consciousness. LZc is a compression algorithm that measures the approximate amount of non-redundant information contained within a string by estimating the minimal size of signal necessary to describe the information contained within the string in a lossless manner. Before applying the LZc algorithm, we discarded data from all electrodes except the 16 sensors present in both participants (Experiment 1) and patients (Experiment 2), and converted our signal into a binary sequence. For every condition, patient and trial separately, we first full-wave rectified the signal and computed the mean evoked response for the particular subject and trial type. Then, for every trial, we assigned a value of '1' to a time point if the trial response was above the mean response for that particular time point, patient, and trial type. If the trial response was contrarily under the mean response, a value of '0' was assigned. This binarized data matrix (observations X trials) was then concatenated observation-by-observation into a single vector, and finally the LZc algorithm determined the size of the dictionary needed to account for the pattern of binary strings observed. As LZc is maximal when data is random, in order to normalize the measure, data on a trial level was randomly shuffled in time, and then the same procedure as with the un-shuffled data was applied. The final estimate of normalized LZc is given as the complexity ratio between the un-shuffled and shuffled data (see Schartner et al., 2017a and Noel et al., 2018c for a similar approach). Of note, LZc is one of the components involved in calculating perturbation complexity index (PCI; Casali et al., 2013), where TMS is applied during EEG recording, then this recording is projected from the sensor space to the neural space by solving the inverse problem, and finally these time series are compressed via LZc (Casali et al., 2013). PCI has been shown to successfully differentiate between patients with distinct DOC diagnoses, while LZc in isolation has been shown to differentiate wakefulness states but not applied in DOC.

2.6.6. Statistical criteria

Cutoff for statistical significance was set at $\alpha < 0.05$ (thus most time-course statistics are reported as " $p < .05$ ") yet to account for the inherent multiple comparisons problem in EEG and the temporal autocorrelation existent in the time-course data we apply a 9.7 ms (5 samples at 512 Hz) contiguous data-point temporal criterion for significance (Guthrie and Buchwald, 1991; see Noel et al., 2018d, and Simon et al., 2017, for a similar approach).

3. Results

3.1. Experiment 1 – healthy participants

3.1.1. Global Field Power

As illustrated in Fig. 2, analysis of GFP demonstrated significant evoked potentials for tactile (101-110 ms post-stimuli onset and 150 ms post-stimuli onset onward), auditory near (at 105-164 ms post-stimuli onset and 177 ms post-stimuli onset onward), auditory far (275 ms post-stimuli onset onward), audiotactile near (117 ms post-stimuli onset onward), and audiotactile far (187 ms post-stimuli onset onward) stimuli (t -tests to zero, all $p < .05$). We next computed the GFP associated with true multisensory presentations (paired conditions, ATnear and ATfar), as well as with conditions with equivalent energies, yet without concurrent multisensory stimulation (summed conditions, Anear + T, and Afar + T; see Cappe et al., 2010 and Noel et al., 2018c, for a similar approach). In order to index whether the co-presentation of stimuli resulted in multisensory integration as a function of distance (near vs. far) - an index of PPS processing - we subtracted the paired response from summed responses for near and far stimulation [i.e., (Anear

+ T) - (ATnear); (Afar + T) - (Afar)] and contrasted these indices across distances via a paired t -test (see Bernasconi et al., 2018, for a similar approach). This data-driven approach showed two time-periods where paired and summed responses differed as a function of distance: 191-238 ms post-stimuli onset (t_1 , highlighted in gray in bottom panel of Fig. 2) and 332-384 ms post-stimuli onset (t_2 , highlighted in gray in the bottom panel of Fig. 2, all $p < .05$). Interestingly, contrasts of each distance to its pre-stimuli baseline (t -test of sum minus pair GFP to zero) demonstrated two significant epochs for the near distance (189-230 ms post-stimuli onset, and 255-449 ms post-stimuli onset), and a sole epoch for the far distance (257 ms post-stimuli onset onward, $p < .05$). The earlier epoch within which only the near distance is different from zero is a case of supra-additivity ($AT > A + T$), while the latter epoch within which both near and far conditions show a multisensory modulation are instances of sub-additivity ($AT < A + T$). Taken together, hence, GFP results demonstrate two time-periods wherein multisensory responses are different from the linear addition of sensory energies, which is further modulated by distance; a PPS effect.

3.1.2. Event-related potentials

The GFP analysis reduced the potential state-space of analysis from 64 electrodes to a sole time-series and identified time-periods of interest. Hence, in the ERP analysis we focused on time periods between 191 and 238 ms and 332-384 ms post-stimuli onset in order to identify electrodes of interest. As illustrated in Fig. 3, and as expected, the scalp distribution of voltages during AT presentation within these time-periods was centro-parietal (top two panels). The contrast between AT presentations when auditory information was presented near (top row) vs. far (middle row) revealed about 15-20 electrodes demonstrating a significant effect within the time-periods of interest (Fig. 3, bottom row). Two of these electrodes, C4 and CP4, were common across time-periods (t_1 and t_2) and across participant's and patient's montages (see Fig. 1 for montages, and Fig. 4 for illustration of electrodes C4 and CP4).

Accordingly, we averaged across electrodes C4 and CP4 and examined the evoked responses at these electrodes. This analysis serves as a normative model for what ought to be expected as the correlate of PPS in these electrodes (which contribute to the global effect as indexed via the GFP analysis). A one-sample t -test to zero revealed significant changes from baseline due to tactile (between 82 and 169 ms post-stimuli onset and 222 ms post-stimuli onset and onward, $p < .05$), auditory near (between 172 and 192 ms post-stimuli onset and 222 ms post-stimuli onset and onward, $p < .05$), auditory far (between 99 and 152 ms post-stimuli onset and 193 ms post-stimuli onset and onward, $p < .05$), audio-tactile near (between 76 and 89 ms post-stimuli onset and 160 ms post-stimuli onset and onward, $p < .05$) and audio-tactile far (between 99 and 150 ms post-stimuli onset and 179 ms post-stimuli onset and onward, $p < .05$) presentations (Fig. 4, top row). Further, when contrasting paired vs. summed responses (Fig. 4, bottom row), a paired-samples t -test demonstrated a significant multisensory effect between 138 and 240 ms post-stimuli onset and 263-453 ms post-stimuli onset in the near condition, and between 257 ms post-stimuli onset and onward for the far condition. The early effect in the near condition was supra-additive (mean between 138 ms-240 ms = 0.55 μ V, S.E.M = 0.18 μ V, t -test to zero, $t = 2.97$, $p = .009$), while the later effect in the near condition and the effect in the far condition were both sub-additive (near condition, mean between 263 ms-453 ms = 0.79 μ V, S.E.M = 0.19 μ V, t -test to zero, $t = 4.14$, $p = 8.64e-4$; far condition, mean between 257 ms-500 ms = 1.01 μ V, S.E.M = 0.24 μ V, t -test to zero, $t = 4.13$, $p = 8.61e-4$, Fig. 4E). Interestingly, the supra-additivity was seemingly driven by a shift in the latency of response (see Fig. 4D); the major positive deflection starting around 145 ms (S.E.M = 8.6 ms) post-stimuli onset in the paired condition and around 184 ms (S.E.M = 11.85) post-stimuli onset in the summed condition (determined as the peak of the second numerical derivative of the time-course; paired t -tests between latencies, $t = 2.66$, $p = .01$). The direct

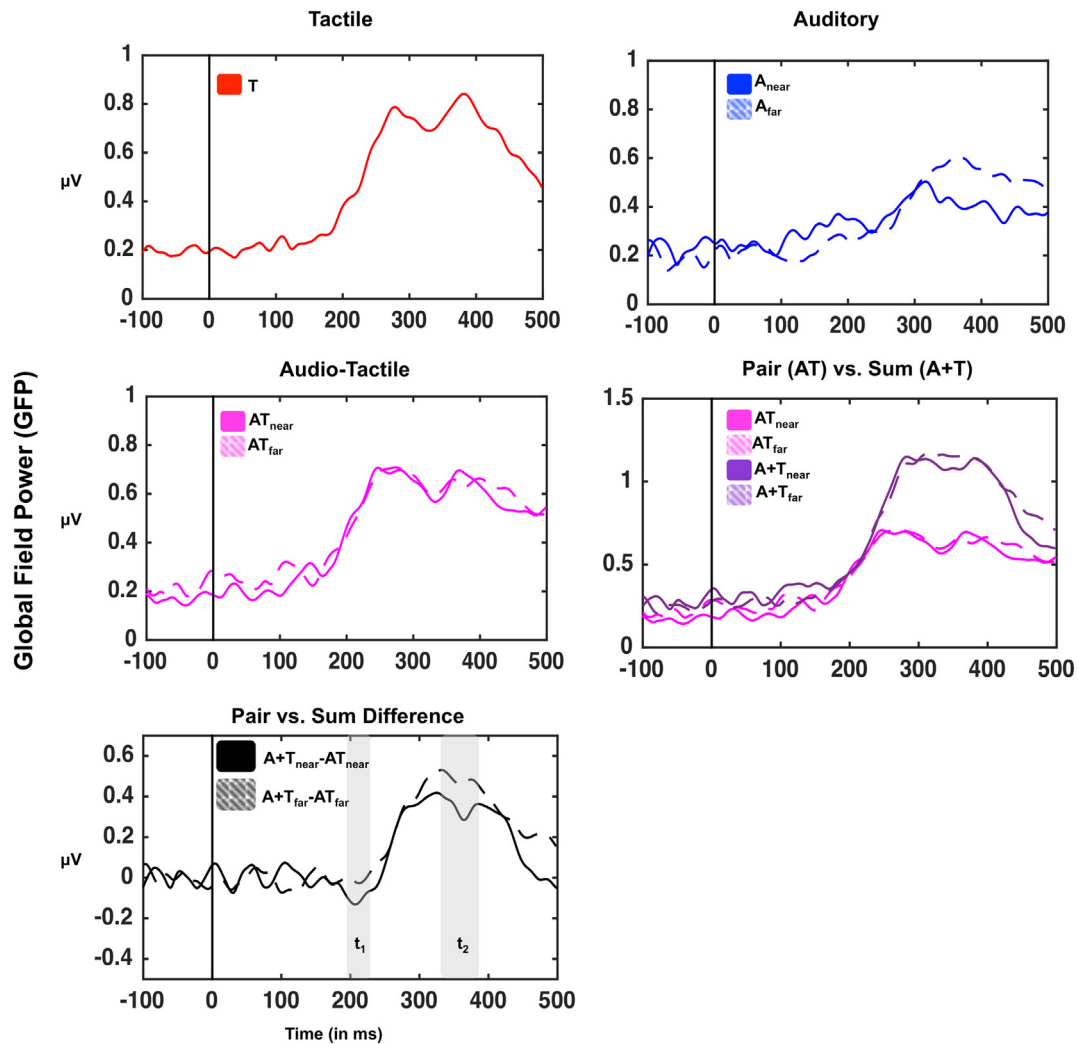


Fig. 2. Global Field Power (GFP) in healthy participants as a function of sensory stimulation. GFP (spatial standard deviation over all electrodes) was calculated for every participant and sensory stimulation condition and then averaged across participants. Sensory stimulation evoked a significant deviation in GFP with respect to baseline for all conditions; tactile (red), auditory (blue; continuous = near; dashed = far), and audio-tactile (light purple; continuous = near; dashed = far). Further, mean voltages for auditory and tactile conditions (at the same distance) were summed and the GFP of this artificial condition was computed in order to contrast the paired GFP (audio-tactile condition; AT) with a summed condition (A + T; dark purple). The difference between paired and summed conditions is shown in the bottom-most panel (black continuous = difference GFP in the near condition; black dashed = difference GFP in the far condition). Differences GFP demonstrated two time-periods of interest. Between 191 and 238 ms post-stimuli onset the difference GFP between paired and summed stimuli for the near condition was significantly different from zero (no difference) and from the difference evoked in the far condition. Secondly, between 332 and 384 ms post-stimuli onset, the difference GFPs for both near and far stimulations were significantly different from zero.

contrast between the multisensory effect (i.e., summed response – paired response) as a function of distance via a paired t-test showed two time-periods where these differed, between 156 ms and 261 ms post-stimuli onset (driven by the supra-additivity present in the near condition solely) and between 330 ms and 382 ms post-stimuli onset (driven by the sub-additive effect present in both near and far conditions).

3.1.3. Topographical dissimilarity

Taking advantage of the fact that a full-montage was recorded in healthy participants, and in an effort to provide an entire picture regarding audio-tactile peri-arm neural encoding, we assessed the topography of voltages across paired and summed evoked potentials (note this analysis is not possible in patients due to their limited sensory coverage). A 2 (pair vs. sum) x 2 (near vs. far) non-parametric TANOVA (Murray et al., 2008), demonstrated a significant main effect of sensory stimulation (52–97 ms post-stimuli onset, and 120 ms post-stimuli onset onward), as well as a main effect of distance (99–128 ms post-stimuli

onset and 474 ms post-stimuli onset and onward). Further, the interaction between these variables was significant (between 30 and 69 ms post-stimuli onset and between 85 and 155 ms post-stimuli onset), arguing that not solely multisensory vs. the sum of unisensory responses evokes differential neural patterns, but further, that multisensory stimuli engage different neural networks as a function of their relative distance to the body. Back projecting average neural pattern templates onto subjects and conditions specified that map 1 (Fig. 5, top right, red) was present for a longer duration in the ATnear condition (M = 126 ms) than in any other condition (ATfar, M = 51 ms; A + Tnear, M = 30 ms; A + Tfar = 54 ms), which resulted in a significant main effect of sensory stimuli condition (pair vs. sum, $p = .01$), as well as a significant interaction between sensory stimulation and distance ($p = 2.0e-4$), but not in a main effect of distance ($p = .76$). Contrarily, map 2 (Fig. 5, second row right column, gray) was present for a shorter duration in the ATnear condition (M = 7 ms) than in the ATfar (M = 50 ms), A + Tnear (M = 71 ms), A + Tfar (M = 61 ms) conditions. Similarly to the case of map 1, this pattern of results for map 2 resulted in a

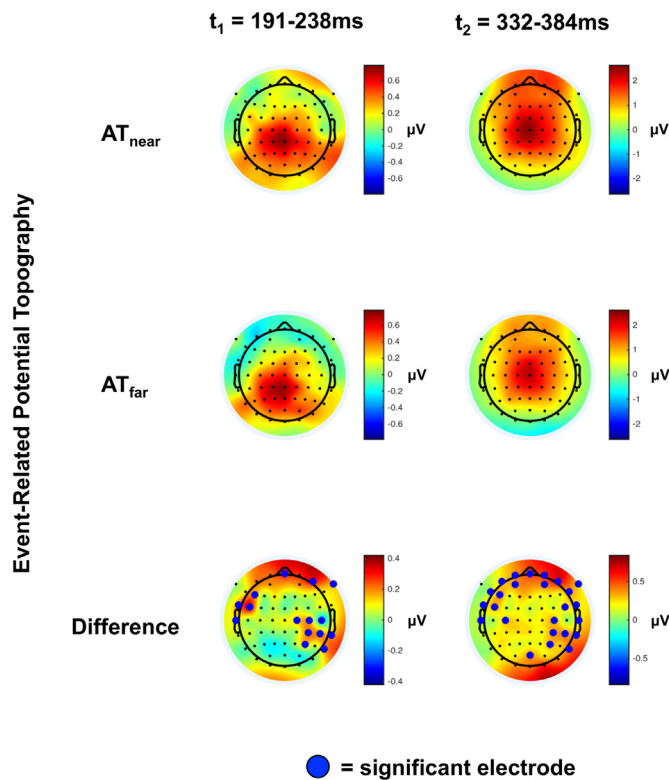


Fig. 3. Topographic representation of voltages during time-periods of significant GFP difference between near and far conditions. AT ERPs (near = top; far = bottom) during 191–238 ms (t1) and 332–384 ms (t2) post-stimuli onset demonstrate a centro-parietal distribution at the scalp level. Bottom panel shows the sensor-wise difference between ATnear and ATfar, and electrodes highlighted by a green dot are significantly different between ATnear and ATfar conditions. Two electrodes (C4 and CP4) show significant differences between distances in both time-periods (t1 and t2), and are also present in DOC patients (see Fig. 1, bottom left), and hence ERP analysis is focused on these electrodes.

significant main effect of sensory stimulation ($p = .02$), as well as in a significant interaction ($p = .007$), but not in a main effect of distance ($p = .59$). Lastly, the presence of map 3 in paired conditions (Fig. 5, third row right column, blue) and map 4 in summed conditions (Fig. 5, fourth row right column, green) differentiated between these experimental manipulations (main effect of sensory stimulation, $p = 4e-4$ and $p = 1e-3$, respectively), but did not show a significant interaction (all $p > .38$), and thus did not bifurcate between peri- and extra-personal space.

3.1.4. Neural complexity

On average, the normalized neural complexity associated with evoked responses in healthy participants was 0.28 (S.E.M = 3.3e-04) and demonstrated a remarkably limited variance (range = 0.278–0.298). A one-way ANOVA suggested there was no difference in evoked LZc across sensory stimulation conditions ($p = .08$, see Fig. 6A, black error bars).

3.2. Experiment 2 –DOC and CMD patients

3.2.1. Event-related potentials

As illustrated in Fig. 6 (top row), on average an ERP response to audio-tactile stimuli was discernable in patients during t1 when auditory stimuli were presented near (averaged across the epoch; $M = 0.97 \mu V$, t-test to zero, $t = 2.21$, $p = .035$), but not far ($M = 0.14 \mu V$, t-test to zero, $t = 0.29$, $p = .77$). During t2, an evoked audio-tactile response was evidenced both when auditory stimuli were presented near ($M = 1.13 \mu V$, t-test to zero, $t = 3.49$, $p = .001$) and far

($M = 1.24 \mu V$, t-test to zero, $t = 2.50$, $p = .017$). The PPS effect described in Experiment 1 ($[(\text{Anear} + T) - \text{ATnear}] - [(\text{Afar} + T) - \text{ATfar}]$ - interaction between pair vs. sum as a function of distance) - was significant in DOC/ putative CMD patients during t1 ($p = .048$; analogous to Fig. 6, second row, left panel, red being different from zero) but not t2 ($p = .92$; Fig. 6, second row, right panel, black). Interestingly, direct comparison of the PPS effect in patients vs. healthy participants (Experiment 1 vs. Experiment 2) was not significant during t1 ($t = 0.06$, $p = .94$), nor t2 ($t = 0.54$, $p = .58$). Thus, while evoked responses were variable, overall DOC/ putative CMD patients seemingly demonstrated differential processing for multisensory stimuli presented near vs. far from their body that was similar to the PPS effect present in the healthy participants. A majority of the patients sample - patients that would all be categorized as DOC unless specifically tested for motor-cognitive dissociation, as executed here via the MBT (Pignat et al., 2016) - was in fact composed of patients putatively with CMD (21 out of 30 sessions), and therefore in a last step we examined whether PPS processing was differentially evidenced in putative CMD than DOC patients. Comparison of the PPS effect between these two latter groups demonstrated a significant effect during t1 ($t = 2.13$, $p = .041$), but not t2 ($t = 1.55$, $p = .13$). The differential PPS effect at t1 was driven by the fact that a PPS effect was present in putative CMD patients ($t = 2.23$, $p = .03$), but absent in DOC patients ($t = 1.06$, $p = .32$; Fig. 6, bottom row).

3.2.2. Neural complexity

On average the normalized neural complexity associated with evoked responses in DOC/ putative CMD patients was 0.27 (S.E.M = 0.009). This value did not significantly change as a function of the nature of sensory stimulation, as suggested by the lack of a significant one-way ANOVA ($p = .98$). On the other hand, and as expected given prior work (e.g., Casali et al., 2013), a 2 (groups; patients vs. healthy participants) x 5 (sensory stimulation) mixed-model ANOVA did demonstrate a main effect of group ($p = .043$). The other variables were non-significant (all $p > .21$). Lastly, as illustrated in Fig. 7A it must be highlighted that while the majority of DOC patients had neural complexity (LZc) values below the healthy participants, some patients had values that were comparable with or inclusively above the mean neural complexity of healthy participants, suggesting a big heterogeneity in cortical preservation in this population. This large variability is to be expected given the heterogeneity in DOC patients within the current study (see Participants section), and is exploited in the next section, where consciousness impairment (as diagnosed via clinicians or neural complexity) is correlated with PPS processing. On average, LZc did not differ between CMD and true DOC patients ($t = 0.61$, $p = .54$).

3.2.3. Relation between PPS, clinical assessment and quantitative EEG-derived assessment of consciousness

The central question of the current study is to determine whether individuals at different stages within the DOC spectrum (including potential CMD) may differentially exhibit neural correlates of PPS. Interestingly, a negative correlation was observed between the PPS effect (e.g., $[\text{sum-pair}]_{\text{near}} - [\text{sum-pair}]_{\text{far}}$, and hence further negative values indicating preserved PPS encoding) at time-period t1 (demonstrating multisensory supra-additivity for near AT stimulation) and normalized LZc ($r = -0.42$, $p = .01$, Fig. 7B). That is, the greater neural complexity data a patient exhibited, the more this patient differentiated between uni- and multi-sensory presentations as a function of distance. This relationship did not hold for the later time-period of interest as determined via Experiment 1, but did suggest a similar trend (t2, $r = -0.22$, $p = .24$, Fig. 7C). Interestingly, when performing these correlations again while dividing between putative CMD and DOC patients, results suggest that LZc and the PPS effect correlate at t1 ($r = -0.44$, $p = .04$) and not t2 ($r = -0.15$, $p = .50$) for DOC patients (as above). However, for putative CMD patients we do not observe a significant relation at t1 ($r = -0.45$, $p = .21$), likely due to the relatively small sample (R-value is of similar magnitude as for DOC and

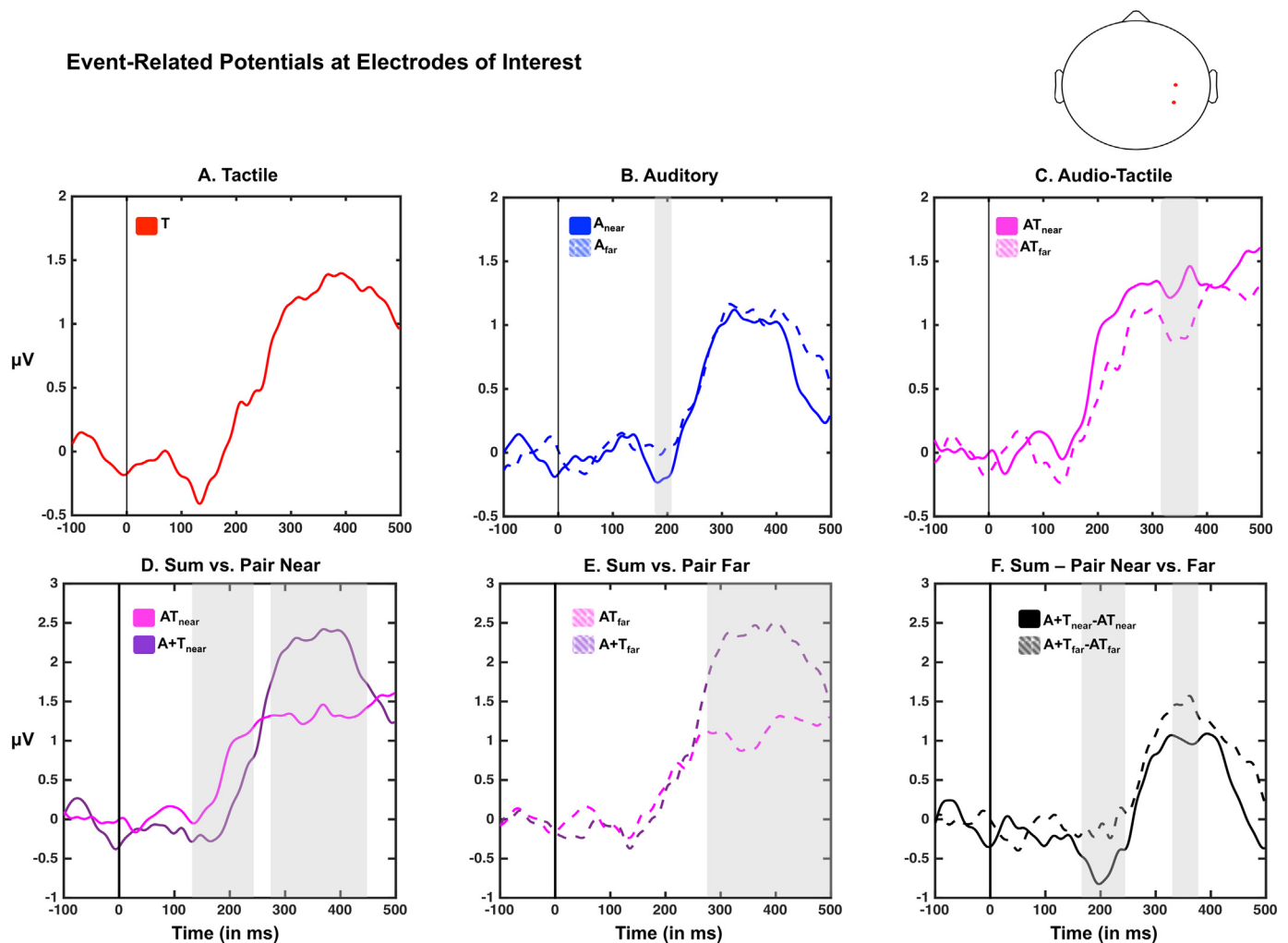


Fig. 4. Event-related potentials in C4/CP4. Top panel illustrates the event-related potential to tactile (red), auditory (blue; continuous = near; dashed = far), and audio-tactile (light purple; continuous = near; dashed = far) at C4/CP4 in healthy participants. Areas shaded in gray demonstrate a significant difference between near and far conditions. Bottom left and center panels illustrate the difference between paired (light purple) and summed (dark purple) ERPs, while the right-most panel demonstrates the multisensory differential as a function of distance; interestingly, a multisensory effect seems present solely in the near condition around 200 ms post-stimulus onset. This difference appears to be due to a latency effect (bottom left panel; positive deflection occurring earlier in the paired than summed activity).

putative CMD patients reported above); we do at t2 ($r = -0.76$, $p = .01$). That is, putatively the lack of correlation at t2 on the overall patient group (DOC+CMD) is due to a different pattern for putative CMD and DOC patients.

Finally, there was a trend for a correlation between the CRS-R scores (clinical measure of consciousness) and neural complexity ($r = 0.30$, $p = .10$, Fig. 7D). However, there was no relationship between CRS-R scores and the PPS measure (t1, $r = -0.09$, $p = .61$; t2 = -0.14 , $p = .45$, Fig. 7E and F, respectively). The correlations between the CRS-R and LZc, as well as between the former and the magnitude of the PPS effect did not change when CMD and DOC patients were analyzed separately (all $p > .07$).

4. Discussion

Neuroimaging techniques have demonstrated that current state-of-the-art clinical assessments of consciousness may misdiagnose patients who retain higher-level cognitive abilities – and thus awareness and supporting a diagnosis of CMD – as within the DOC spectrum (Owen et al., 2006; Monti et al., 2010). In turn, in the last decade neural predictors of preserved consciousness have been proposed (Faugeras et al., 2012; King et al., 2013; Tzovara et al., 2015; see Giacino et al.,

2014, and Laureys and Schiff, 2012, for reviews). In contrast to these previous reports – some employing a rather engineering-like than scientific approach – here we propose to use a low-level multisensory stimulation paradigm arguably tapping into a primordial (Graziano and Cooke, 2006) and very specific sensorimotor network, i.e., the PPS network. The PPS is a multisensory-motor space mediating self-environment interaction (Serino, 2019) for defense or approach behavior (Clery et al., 2015). Thus, evidence for a representation of this space in DOC and/or CMD patients would be evidence for the presence of sensorimotor systems ready to interact with external objects (which further can be molded by intentionality) and putatively for a primitive form of self-awareness (Blanke, 2012; Blanke et al., 2015; Noel et al., 2018b). Overall, results demonstrate that PPS processing is widely varying in patients within the DOC spectrum (as assessed via the CRS-R). Importantly, the multisensory representation of this space is seemingly graded with EEG complexity, and remains present in patients potentially with CMD, but appears degraded in DOC patients. In turn, when arguably controlling for motor output (equivalent between CMD and DOC), the PPS metric seemingly can differentiate between those capable and incapable of motor intent.

In a first step we established the “normative model” of PPS representation by assessing the EEG correlates of audio-tactile integration

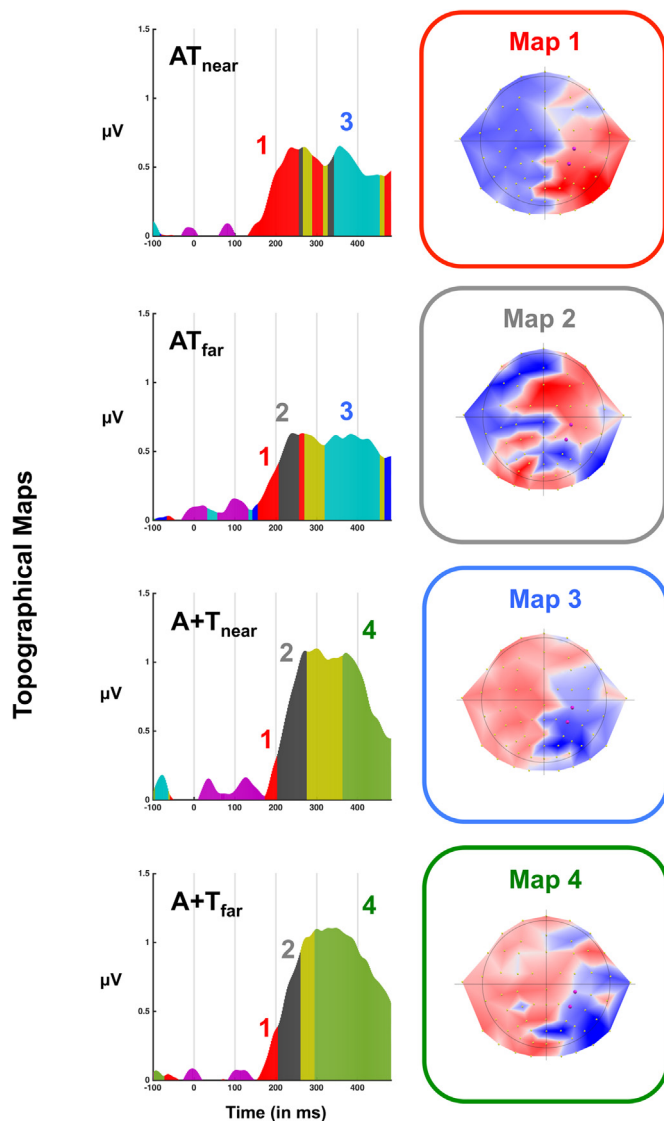


Fig. 5. Topographical maps. Topographic cluster analysis identified a restricted number of maps that could account for the topographical distributions present during audio-tactile processing of stimuli both in the near and far space. Interestingly, map 1 (red, right panel) was present for all conditions (from top to bottom; audio-tactile near; audio-tactile far; audio + tactile near; audio + tactile far) but was short-lived for all conditions except for audio-tactile near; the peri-personal space condition. In the rest of conditions, map 1 was replaced by map 2 (gray, right panel). A second clear distinction existed between conditions: map 3 (blue, right panel) was present at large delays in multisensory conditions (audio-tactile near and audio-tactile far), while instead map 4 (green, right panel) was present in summed conditions.

for near vs. far stimuli in healthy subjects. This step is novel and important as audio-tactile PPS has only been electrophysiologically probed in humans via intracranial recordings in epileptic patients – not at the scalp-level – and around the trunk (vs. hand; Bernasconi et al., 2018). GFPs for the summed condition (i.e., auditory + tactile) were constructed and compared to the multisensory condition (i.e., audio-tactile) to determine time-periods of multisensory non-linearity (Bernasconi et al., 2018; Noel et al., 2018c; Noel et al., 2019). This analysis revealed the presence of a supra-additive effect 191 to 238 ms post-stimuli onset, solely when auditory and tactile stimulation were presented in close spatial proximity; namely, a PPS effect. A further dissociation between near and far spaces occurred between 332 and 384 ms post-stimuli onset. However, in this second case both conditions demonstrated a sub-additivity with regard the linear unisensory

summation model. Electrodes driving the GFP multisensory space-specific difference were located in centro-parietal areas, in line with location of PPS-related processing from neuroimaging studies (Grivaz et al., 2017). Lastly, not only did the strength of neural generators differ, but also their spatial configuration. These findings mimic prior evidence for EEG-based supra-additive effects (e.g., Sperdin et al., 2010; although arguably these are the minority vis-à-vis sub-additive effects) and are well in line with the spatial principle of multisensory integration (Murray and Wallace, 2012). Most importantly, these results demonstrate a PPS effect with a similar latency to the sole other electrophysiological study recording neural response to audio-tactile stimulation within vs. outside the PPS (with intracranial recording; Bernasconi et al., 2018).

Having restricted the analyses in time (191–238 ms and 332–384 ms post-stimuli onset) and space (C4/CP4) based on the experiment with healthy participants, we explored evoked-potentials in DOC patients (as classified via CRS-R) during the presentation of tactile, auditory, and audio-tactile stimulation in peri- and extra-personal space. Group averaged responses were modest, which is to be expected in relatively older participants and when averaging across patients with different diagnoses and even different etiologies within a diagnostic category. Importantly, nonetheless, the patients' average did indicate a multisensory effect (sum condition different from pair) that was space-dependent. Interestingly, this PPS effect in patients was present in the first time-period analyzed (where it was not different from the effect present in healthy controls; T1 = 191–238 ms post-stimuli onset), but was absent at the later latency (T2 = 332–384 ms post-stimuli onset). Further bifurcation of the patient group into putative CMD and DOC patients revealed that the PPS effect during T1 present in DOC/ putative CMD group was specifically driven by the putative CMD patients, and was absent in DOC non-CMD patients.

Given that PPS processing was seemingly present in patients with varying degrees of motoric/awareness impairments, we attempted to relate PPS encoding to both a clinical assessment and LZc, a measure of complexity previously associated with consciousness (Schartner et al., 2015). The PPS measure correlated with an index of EEG complexity, a component of the PCI which associated with TMS has been shown to successfully differentiate comatose, VS/UWS, MCS, and healthy participants (Casali et al., 2013) or in isolation to characterize healthy participants under anesthesia. Interestingly, neither EEG complexity, nor the PPS measure showed a significant correlation with clinical assessment of different states of DOC, based on CRS-R. We consider this a strength of the current study, and not a limitation, as misdiagnoses (or at least the limited prognostic value of clinical assessments) in allegedly DOC patients are well documented (Cruse et al., 2012). That is, it was precisely our objective here to characterize PPS across a wide spectrum of DOC diagnoses and complement clinical evaluations with a neuroimaging-based evaluation for the potential for human-environment interactions and self-awareness. If clinical evaluations and EEG-derived indexing of PPS would demonstrate a perfect correlation, there would be no added value from the latter to the former. Similarly, while LZc and the EEG-derived measure of PPS both discriminated patients from healthy controls and correlate at T1, these two measures also showed discrepant behavior. LZc showed a trend to correlate with the CRS-R scale ($p = .10$), while the PPS measure did not. Moreover, and perhaps most notably, PPS encoding differentiated between putative CMD and non-CMD patients, while LZc did not. Together, this pattern seemingly indicates that while LZc might identify DOC, it is not an unequivocal index of consciousness-level. Namely, putative CMD and non-CMD patients arguably have different levels of consciousness, yet LZc was not able to differentiate between these groups. In counterpart, the EEG-derived measure of PPS was able to dissociate between putative CMD and non-CMD patients, thus PPS encoding captures potential motor intention, but not unequivocally consciousness level per se. The current results, therefore, support the clinical assessment made based on MBT as complementary to the CRS-R (Pincherle et al., 2018) and support the

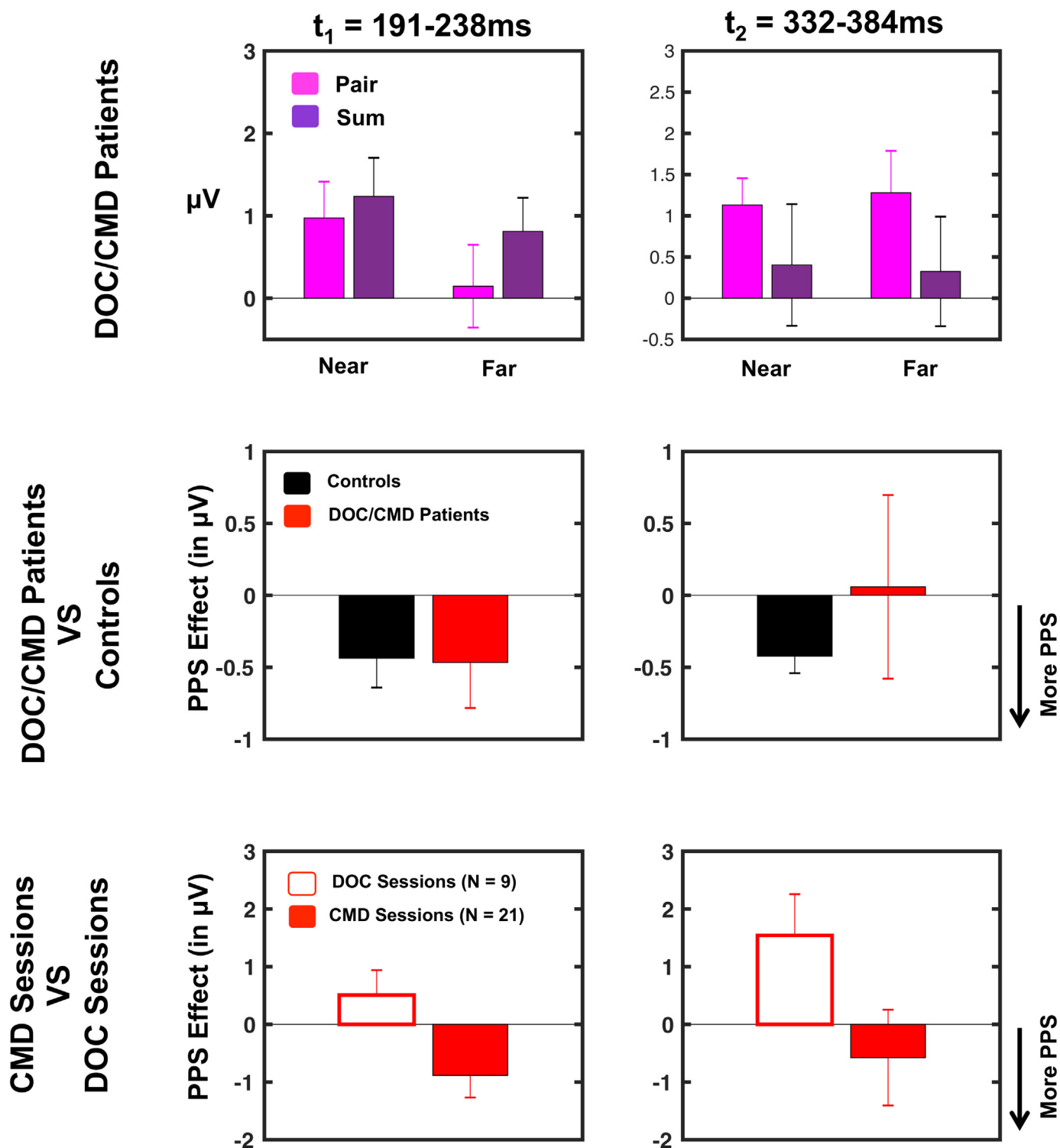


Fig. 6. EEG-based metric of PPS in *CMD* patients. Top row; based on results from Experiment 1 we restricted analyses to electrodes C4/CP4 (averaged) and time periods t1 (191-238ms post-stimuli onset) and t2 (332-384 ms post-stimuli onset). Within this constrained spatio-temporal space we measured activity evoked to audio-tactile stimulation (pair = pink), as well as to the sum of auditory and tactile stimulation (sum = dark purple). Overall, significant audio-tactile responses were discernable during t1 and t2 (sole exception being responses during t1 when auditory stimulation was presented far). Middle row; the PPS effect ($[(A_{near} + T) - AT_{near}] - [(A_{far} + T) - AT_{far}]$, negative values indicating a PPS effect given Experiment 1) was evaluated both at t1 and t2 in *CMD* patients (red, of note, this included *DOC*+*CMD* patients, that is, patients classified as *DOC* according to the CRS) and contrasted to control subjects (black). Interestingly, there was no difference in PPS effect between patients and controls, suggesting that a significant PPS effect was present in *CMD* patients (particularly for t1, t2 showed no difference between *CMD* and controls given the large variance in *CMD* patients; see middle row, second column, red). Bottom row; Lastly *CMD* patients were contrasted to “true” *DOC* patients. This analysis indicated a differential PPS processing in *CMD* (filled red) and *DOC* (white, red outline) participants during t1 (left column) but not t2 (right column). Error bars represent ± 1 S.E.M.

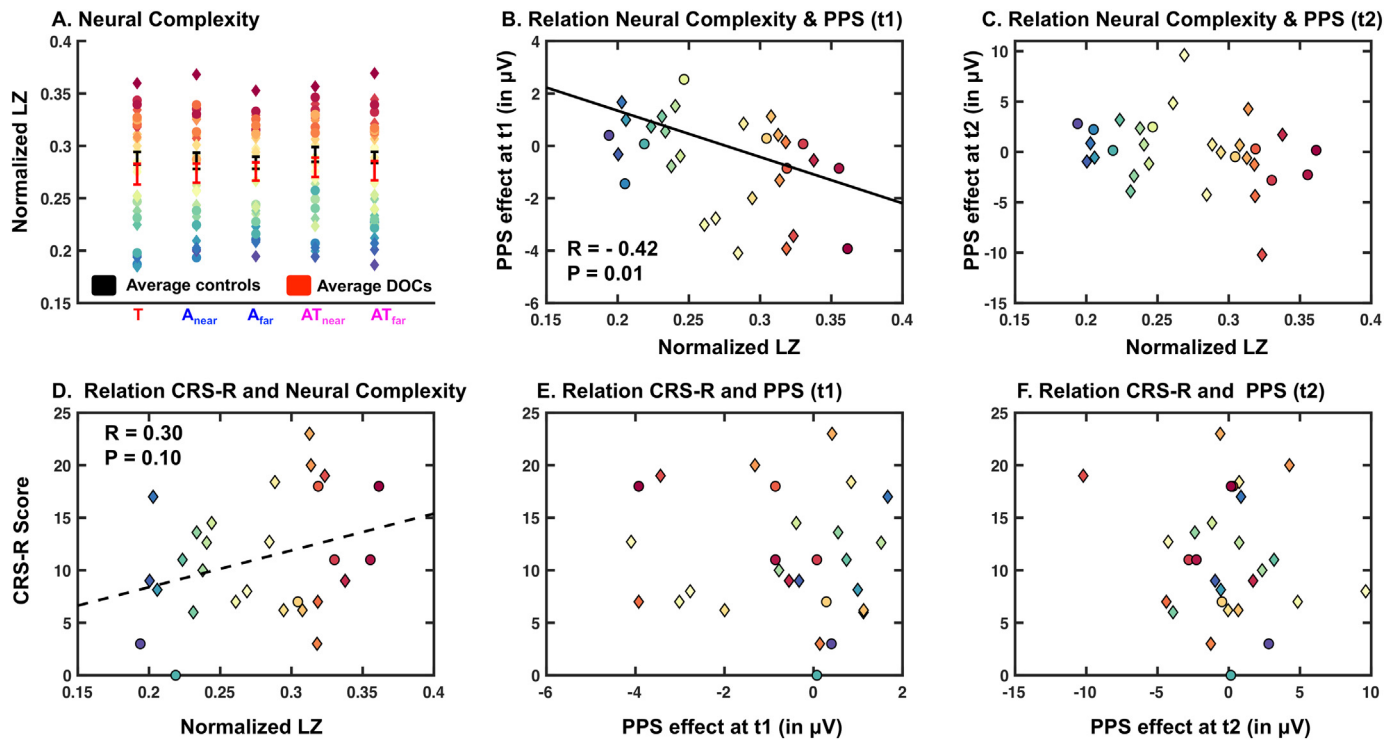


Fig. 7. Contrast of PPS effect measured in DOC patients with Lempel-Ziv complexity (LZc) and clinical assessments. A; Top left-most panel shows the average normalized LZc computed in healthy control participants (Experiment 1; black) and in DOC patients (Experiment 2; red) as a function of sensory stimulation (Tactile = red; audio near = first blue; audio far = second blue; audio-tactile near = first purple; audio-tactile far = second purple). Further, individuals subject data (color coded from most to least complex averaged across sensory stimulation conditions) is shown for patients, which surprisingly show that while on average patients show less LZc, there are DOC patients with higher than average LZc. B; Significant correlation ($r = -0.42$, $p = .01$) between the PPS effect (average voltage at C4/CP4 for [(A + Tnear) – ATnear]– (A + Tfar) – ATfar); negative values indicating a PPS effect) and normalized LZc at time-period t1. C; Same as B, for time-period t2; this time period not showing a significant correlation. D; Correlation between the (full) clinical assessment of consciousness – Coma Recovery Scale (CRS-R) – and normalized LZc, a neurophysiological measure of consciousness. These measures are not significantly correlated, demonstrating somewhat of a discrepancy between bedside assessments reliant on behavioral output and neurophysiological measurements. E and F; There was no correlation between the PPS measure and behavioral assessments of consciousness. Putative *CMD* patients are depicted via diamonds, while non-*CMD* patients (i.e., “true” DOC) are shown as circles.

PPS index as an objective measure of *CMD*. Extensive validation with larger samples may in the future validate the current PPS-EEG marker as either a complementary clinical measure of *DOC* severity, particularly by indexing potential residual motor intention, or as in itself a good measure of consciousness-level.

Neural complexity, used in conjunction with transcranial magnetic stimulation, has been shown to successfully differentiate across distinct levels of consciousness (PCI; Casali et al., 2013). It will be interesting to examine whether perturbation complexity index (see above, Casali et al., 2013), at difference from LZc, can differentiate between *CMD* and non-*CMD* patients. Finally, as alluded to above, here we show that PPS processing can highlight potential residual cognition/motor intention. In turn, just as the MBT scale complements the CRS-R, seemingly this EEG-based metric of PPS can complement other neuroimaging techniques aimed at indexing consciousness, such as PCI or LZc. Nonetheless, it is notable that these two EEG approaches are conceptually very different. Arguably, PCI and LZc have more of an engineering than a scientific flavor. On the other hand, the delineation of PPS counts with a well-established scientific history; the PPS is known to be encoded by multisensory neurons with depth restricted receptive fields (Graziano and Cooke, 2006) and to remap as a function of human-environment interactions (Serino et al., 2017; Noel et al., 2015b, 2018b). Further, the PPS is taken to reflect self-location (Noel et al., 2015b; Salomon et al., 2017) and has been directly linked to body ownership (Blanke et al., 2015; Noel et al., 2018b), two key components of bodily self-consciousness (Blanke and Metzinger, 2009; Blanke, 2012). Indeed, it has been proposed that the multisensory integration of body-related information within the PPS is at the basis of a primitive form of self-

awareness (Blanke, 2012; Blanke et al., 2015; Serino, 2016, 2019; Noel et al., 2018b). Thus, by demonstrating a PPS representation that is graded with the level of consciousness (as shown here), and present in patients potentially with *CMD*, but not “true” *DOC*, it may be suggested that at least a portion of these patients retain a minimal form of self-awareness, that is linked to one’s own body. This focus on a minimal and bodily-ground selfhood differentiates the current attempt to map PPS in *DOC* patients from classic approaches to the study of consciousness that emphasize awareness of external events without specific reference to the self.

In conclusion, here we develop a neuroimaging-based PPS metric in healthy individuals and demonstrate that applied to *DOC* patients this meter scales with an EEG-based proxy of consciousness, but not with standard clinical assessments of consciousness. Further, putative *CMD* patients, but not true *DOC* patients, evidenced PPS processing. Hence, the findings indicate that certain “*DOC* patients” are capable of multi-sensory integration, which is itself modulated by the spatial proximity of the external stimuli. Arguably, this finding supports the fact that certain patients routinely diagnosed as within the *DOC* spectrum (i.e., *CMD* patients) have the capacity to recruit a neural system that underlies a multisensory-motor representation of the space where the body interacts with the environment, and they are putatively inclusively capable of a minimal form of self-awareness (Blanke, 2012; Blanke et al., 2015). This observation supports recent fMRI and EEG evidence (Edlow et al., 2017; Braiman et al., 2018) indicating that *CMD* patients have greater cognitive capacities than what can be observed at bedside with standard behavioral scales (Wade, 2018). Furthermore, our findings provide further support for the classification of *CMD* based

on the MBT. In comparison to other neurophysiological/neuroimaging investigations, indexing PPS in these patients may be applicable in the acute phase and most importantly is independent from command following, motor responses, and vigilance fluctuations. Clinically, these results highlight the importance of providing neurorehabilitation opportunities to patients deemed as within the DOC spectrum according to the CRS-R, as these patients may mainly need training in motor functions to regain full capacities, as opposed to needing to regain consciousness.

Contributions

J.P.N. designed research, performed research, analyzed data, and wrote the paper. C.C. designed research and wrote the paper. S. P. performed research and contributed tools. J.J. performed research and contributed tools. M.L.D.S. performed research. P. R., performed research. M.D.L. designed research and contributed tools. J.d.R.M. designed research and contributed tools. K.D. designed research and wrote the paper. A.S. designed research and wrote the paper.

Declaration of Competing Interest

The authors declare no competing financial interests.

Acknowledgments

The authors acknowledge the neurorehabilitation staff at CHUV for their help in completing this project. This study was supported by a grant from the Swiss National Foundation [PP00P3_163951/1], and by the Fondation Biaggi (Lausanne, Switzerland) to AS.

References

- Andrillon, T., Poulsen, A.T., Hansen, L.K., Lger, D., Kouider, S., 2016. Neural markers of responsiveness to the environment in human sleep. *J. Neurosci.* 36, 6583–6596.
- Avillac, M., Ben Hamed, S., Duhamel, J.R., 2007. Multisensory integration in the ventral intraparietal area of the macaque monkey. *J. Neurosci.* 27 (8), 1922–1932. <https://doi.org/10.1523/JNEUROSCI.2646-06.2007>.
- Bernasconi, F., Noel, J.-P., Park, H., et al., 2018. Audio-tactile and peripersonal space processing around the trunk in human parietal and temporal cortex: an intracranial EEG study. *bioRxiv* 249078.
- Bernat, J., 2006. Chronic disorders of consciousness. *Lancet* 367, 1181–1192.
- Birbaumer, N., Ghanayim, N., Hinterberger, T., Iversen, I., Kotchoubey, B., Kubler, A., et al., 1999. A spelling device for the paralysed. *Nature* 398 (6725), 297.
- Blanke, O., 2012. Multisensory brain mechanisms of bodily self-consciousness. *Nat. Rev. Neurosci.* 13, 556–571.
- Blanke, O., Metzinger, T., 2009. Full-body illusions and minimal phenomenal selfhood. *Trends Cogn. Sci.* 13, 7–13.
- Blanke, O., Slater, M., Serino, A., 2015. Behavioral, neural, and computational principles of bodily self-consciousness. *Neuron* 88, 145–166.
- Braiman, C., Fridman, E.A., Conte, M.M., Voss, H., Reichenbach, C.S., Reichenbach, T., Schiff, N.D., 2018. Cortical response to the natural speech envelope correlates with neuroimaging evidence of cognition in severe brain injury. *Curr. Biol.* <https://doi.org/10.1016/j.cub.2018.10.057>.
- Brozzoli, C., Gentile, G., Ehrsson, H.H., 2012. That's near my hand! Parietal and premotor coding of hand-centered space contributes to localization and self-attribution of the hand. *J. Neurosci.* 32 (42), 14573–14582.
- Canzoneri, E., Magosso, E., Serino, A., 2012. Dynamic sounds capture the boundaries of peripersonal space representation in humans. *PLoS One* 7 (9), e44306. <https://doi.org/10.1371/journal.pone.0044306>.
- Cappe, C., Thut, G., Romei, V., Murray, M.M., 2010. Auditory-visual multisensory interactions in humans: Timing, topography, directionality, and sources. *J. Neurosci.* 30, 12572–12580.
- Casali, A.G., et al., 2013. A theoretically based index of consciousness independent of sensory processing and behavior. *Sci. Transl. Med.* 5 (198ra105–198ra105).
- Clery, J., Guipponi, O., Wardak, C., et al., 2015. Neuronal bases of peripersonal and extrapersonal spaces, their plasticity and their dynamics: knowns and unknowns. *Neuropsychologia* 70, 313–326.
- Cruse, D., Chennu, S., Chatelle, C., Bekinschtein, T.A., Fernandez-Espejo, D., Pickard, J.D., et al., 2012. Bedside detection of awareness in the vegetative state: a cohort study. *Lancet* 378, 2088–2094.
- Curley, W.H., Fargacs, P.B., Voss, H.U., Conte, M.M., Schiff, N.D., 2018. Characterization of EEG signals revealing covert cognition in the injured brain. *Brain* 141 (5), 1404–1421. <https://doi.org/10.1093/brain/awy070>.
- Delorme, A., Makeig, S., 2004. EEGLAB: an open source toolbox for analysis of single-trial EEG dynamics including independent component analysis. *J. Neurosci. Methods* 134, 9–21. <https://doi.org/10.1016/j.jneumeth.2003.10.009>.
- Edlow, B.L., Chatelle, C., Spencer, C.A., Chu, C.J., Bodien, Y.G., O'Connor, K.L., Hirschberg, R.E., Hochberg, L.R., Giacino, J.T., Rosenthal, E.S., Wu, O., 2017. Early detection of consciousness in patients with acute severe traumatic brain injury. *Brain* 140 (9), 2399–2414.
- Faugeras, F., Rohaut, B., Weiss, N., Bekinschtein, T., Galanaud, D., Puybasset, L., et al., 2012. Event related potentials elicited by violations of auditory regularities in patients with impaired consciousness. *Neuropsychologia* 2012 (50), 403–418.
- Giacino, J.T., Kalmar, K., Whyte, J., 2004. The JFK Coma Recovery Scale-Revised: measurement characteristics and diagnostic utility. *Arch. Phys. Med. Rehabil.* 85 (12), 2020–2029. 15605342.
- Giacino, J.T., Schnakers, C., Rodriguez-Moreno, D., Kalmar, K., Schiff, N.D., Hirsch, J., 2009. Behavioral assessment in patients with disorders of consciousness: gold standard or fool's gold? *C. Elsevier* 177, 33–48.
- Giacino, J.T., Fins, J.J., Laureys, S., Schiff, N.D., 2014. Disorders of consciousness after acquired brain injury: The state of the science. *Nat. Rev. Neurol.*, vol. 10 (2), 99–114 (2014).
- Graziano, M.S., Cooke, D.F., 2006. Parieto-frontal interactions, personal space, and defensive behavior. *Neuropsychologia* 44 (13), 845–859.
- Graziano, M.S.A., Reiss, L.A., Gross, C.G., 1999. A neuronal representation of the location of nearby sounds. *Nature* 397, 428–430.
- Graziano, M.S., Cooke, D.F., Taylor, C.S., 2000. Coding the location of the arm by sight. *Science* 290, 1782–1786.
- Grivaz, P., Blanke, O., Serino, A., 2017. Common and distinct brain regions processing multisensory bodily signals for peripersonal space and body ownership. *Neuroimage* 147, 602–618.
- Guthrie, D., Buchwald, J.S., 1991. Significance testing of difference potentials. *Psychophysiology* 28, 240–244.
- King, J.R., Sitt, J.D., Faugeras, F., Rohaut, B., El Karoui, I., Cohen, L., et al., 2013. Information sharing in the brain indexes consciousness in noncommunicative patients. *Curr. Biol.* 23, 1914–1919.
- Koenig, T., Melie-Garcia, L., 2010. A method to determine the presence of averaged event-related fields using randomization tests. *Brain Topogr.* 23, 233–242.
- Koenig, T., Kottlow, M., Stein, M., Melie-Garcia, L., 2011. Ragú: a new tool for the analysis of EEG and MEG event-related scalp field data using global randomization statistics. *Comput. Intell. Neurosci.* 2011, 93892.
- Laureys, S., Schiff, N.D., 2012. Coma and consciousness: Paradigms (re)framed by neuroimaging. *NeuroImage* 61 (2), 478–491 (2012).
- Laureys, S., Owen, A.M., Schiff, N.D., 2004. Brain function in coma, vegetative state, and related disorders. *Lancet Neurol.* 3, 537–546. [https://doi.org/10.1016/S1474-4422\(04\)00852-X](https://doi.org/10.1016/S1474-4422(04)00852-X).
- Laureys, S., Celesia, G.G., Cohadon, F., Lavrijsen, J., Leon-Carrion, J., Sannita, W.G., et al., 2010. Unresponsive wakefulness syndrome: a new name for the vegetative state or apallic syndrome. *BMC Med.* 8, 68.
- Lehmann, D., Skrandies, W., 1980. Reference-free identification of components of checkerboard-evoked multichannel potential fields. *Electroencephalogr. Clin. Neurophysiol.* 48, 609–621. [https://doi.org/10.1016/0013-4694\(80\)90419-8](https://doi.org/10.1016/0013-4694(80)90419-8).
- Lehmann, D., Ozaki, H., Pal, I., 1987. EEG alpha map series: brain microstates by space oriented adaptive segmentation. *Electroencephalogr. Clin. Neurophysiol.* 67, 271–288.
- Lempel, A., Ziv, J., 1976. On the complexity of finite sequences. *IEEE Trans. Inf. Theory* 22, 75–81.
- Makin, T.R., Holmes, N.P., Brozzoli, C., Rossetti, Y., Farnè, A., 2009. Coding of visual space during motor preparation: approaching objects rapidly modulate corticospinal excitability in hand-centered coordinates. *J. Neurosci.* 29, 11841–11851.
- Maravita, A., Iriki, A., 2004. Tools for the body (schema). *Trends Cogn. Sci.* 8 (2), 79e86 (<http://doi.org/S1364661303003450> [pii]10.1016/j.tics.2003.12.008).
- Matelli, M., Luppino, G., 2001. Parietofrontal circuits for action and space perception in the macaque monkey. *Neuroimage* 14, S27–S32.
- Monti, M.M., Vanhaudenhuyse, A., Coleman, M.R., Boly, M., Pickard, J.D., Tshibanda, L., et al., 2010. Willful modulation of brain activity in disorders of consciousness. *N. Engl. J. Med.* 362, 579–589.
- Murray, M.M., Wallace, M.T., 2012. *The Neural Bases of Multisensory Processes*. CRC Press, Boca Raton, FL.
- Murray, M.M., Brunet, D., Michel, C.M., 2008. Topographic ERP analyses: a step-by-step tutorial review. *Brain Topogr.* 20, 249–264.
- Noel, J.P., Grivaz, D., Marmaroli, P., Lissek, H., Blanke, O., Serino, A., 2015a. Full body action remapping of peripersonal space: the case of walking. *Neuropsychologia* 70, 375–384.
- Noel, J.-P., Pfeiffer, C., Blanke, O., Serino, A., 2015b. Peri-personal space as the space of the bodily self. *Cognition* 114, 49–57.
- Noel, J.P., Samad, M., Doxon, A., Clark, J., Keller, S., Di Luca, M., 2018a. Peri-personal Space as a Prior in Coupling Visual and Proprioceptive Signals. 8. pp. 15819.
- Noel, J.P., Blanke, O., Serino, A., 2018b. From multisensory integration in peripersonal space to bodily self-consciousness: from statistical regularities to statistical inference. *Ann. N.Y. Acad. Sci.* <https://doi.org/10.1111/nyas.13867>.
- Noel, J.P., Simon, D., Thelen, A., Maier, A., Blake, R., Wallace, M., 2018c. Probing electrophysiological indices of perceptual awareness across unisensory and multisensory modalities. *J. Cogn. Neurosci.* 30, 814–828.
- Noel, J.P., Blanke, O., Magosso, E., Serino, A., 2018d. Neural adaptation accounts for the resizing of peri-personal space representation: evidence from a psychophysical-computational approach. *J. Neurophysiol.* <https://doi.org/10.1152/jn.00652.2017>.
- Noel, J.P., Serino, A., Wallace, M., 2018e. Increased neural strength and reliability at the boundary of peri-personal space. *J. Cogn. Neurosci.* https://doi.org/10.1162/jocn_a.01334.
- Noel, J.P., Park, H., Pasqualini, I., Lissek, Wallace, Blanke, M., Serino, O., A., 2018f.

- Audio-visual sensory deprivation degrades visuo-tactile peri-personal space. *Conscious. Cogn.* 61, 61–75.
- Noel, J.P., Ishizawa, Y., Patel, S.R., Eskandar, E., Wallace, M., 2019. Leveraging non-human primate multisensory neurons and circuits in assessing consciousness theory. *BioRxiv*. <https://doi.org/10.1101/584516>.
- Owen, A.M., 2014. Disorders of consciousness: diagnostic accuracy of brain imaging in the vegetative state. *Nat. Rev. Neurol.* 10 (7), 370–371. 24934139.
- Owen, A.M., Coleman, M.R., Boly, M., Davis, M.H., Laureys, S., Pickard, J.D., 2006. Detecting awareness in the vegetative state. *Science* 313, 1402.
- Patane, I., Cardinali, L., Salemmé, R., Pavani, F., Farne, A., Brozzoli, C., 2018. Action planning modulates peripersonal space. *J. Cog Neurosci* 1–14.
- Perrin, F., Pernier, J., Bertrand, O., Giard, M.H., Echallier, J.F., 1987. Mapping of scalp potentials by surface spline interpolation. *Electroencephalogr. Clin. Neurophysiol.* 66, 75–81. [https://doi.org/10.1016/0013-4694\(87\)90141-6](https://doi.org/10.1016/0013-4694(87)90141-6).
- Pfeiffer, C., Noel, J.P., Serino, A., Blanke, O., 2018. Vestibular modulation of peripersonal space boundaries. *Eur. J. Neurosci.* 47, 800–811.
- Pignat, J.M., Mauron, E., Jöhr, J., Gilart de Keranflech, C., Van De Ville, D., Preti, M.G., et al., 2016. Outcome prediction of consciousness disorders in the acute stage based on the complementary motor behavioural tool. *PLoS One* 11, e0156882.
- Pincherle, A., Jöhr, J., Chatelle, C., Pignat, J.M., Du Pasquier, R., Ryvlin, P., Oddo, M., Diserens, K., 2018. Motor behavior unmasks residual cognition in disorders of consciousness. *Ann. Neurol.* 443–447. <https://doi.org/10.1002/ana.25417>.
- Rizzolatti, G., Fadiga, L., Fogassi, L., Gallese, V., 1997. The space around us. *Science* 277, 190–191.
- Salomon, R., Noel, J.P., Lukowska, M., et al., 2017. Unconscious integration of multisensory bodily inputs in the peripersonal space shapes bodily self-consciousness. *Cognition* 166, 174–183.
- Sarasso, S., et al., 2015. Consciousness and complexity during unresponsiveness induced by propofol, xenon, and ketamine. *Curr. Biol.* 25, 3099–3105.
- Schartner, M., et al., 2015. Complexity of multi-dimensional spontaneous eeg decreases during propofol induced general anaesthesia. *PLoS One* 10, e0133532.
- Schartner, M.M., et al., 2017a. Increased spontaneous MEG signal diversity for psychoactive doses of ketamine, LSD and psilocybin. *Sci. Rep.* 7, 46421. <https://doi.org/10.1038/srep46421>.
- Schartner, M.M., et al., 2017b. Global and local complexity of intracranial eeg decreases during nrem sleep. *Neurosci. Conscious.* 3 (1) (niw022).
- Schiff, N.D., 2015. Cognitive motor dissociation following severe brain injuries. *JAMA Neurol.* 72, 1413–1415.
- Serino, A., 2016. Variability in Multisensory Responses Predicts the Self-Space. *Trends Cogn. Sci.* 20 (3), 169–170.
- Serino, A., 2019. Peripersonal space (PPS) as a multisensory interface between the individual and the environment, defining the space of the self. *Neurosci. Biobehav. Rev.* 99, 138–159.
- Serino, A., Annella, L., Avenanti, A., 2009. Motor properties of peripersonal space in humans. *PLoS One* 4, e6582.
- Serino, A., Canzoneri, E., Avenanti, A., 2011. Fronto-parietal areas necessary for a multisensory representation of peripersonal space in humans: an rTMS study. *J. Cogn. Neurosci.* 23, 2956–2967.
- Serino, A., Noel, J.P., Galli, G., Canzoneri, E., Marmaroli, P., Lissek, H., Blanke, O., 2015. Body part-centered and full body-centered peripersonal space representations. *Sci. Rep.* 5, 18603. <https://doi.org/10.1038/srep18603>.
- Serino, A., Noel, J.-P., Mange, R., Canzoneri, E., Pellencin, E., Bello-Ruiz, J., Bernasconi, F., Blanke, O., Herbelin, B., 2017. Peri-personal space: an index of multisensory body-interaction in real, virtual, and mixed realities. *Front. ICT* 4, 31.
- Simon, D.M., Noel, J.P., Wallace, M.T., 2017. Event Related Potentials Index Rapid Recalibration to Audiovisual Temporal Asynchrony. *Front. Integr. Neurosci.* 11, 8.
- Sperdin, H.F., Cappe, C., Murray, M.M., 2010. The behavioral relevance of multisensory neural response interactions. *Front. Neurosci.* 4, 9.
- Teasdale, G., Jennet, B., 1974. Assessment of coma and impaired consciousness: a practical scale. *Lancet* 1, 81–84.
- Tzovara, A., Simonin, A., Oddo, M., Rossetti, A.O., De Lucia, M., 2015. Neural detection of complex sound sequences in the absence of consciousness. *Brain* 138, 1160–1166. <https://doi.org/10.1093/brain/awv041>.
- Wade, D.T., 2018. How often is the diagnosis of the permanent vegetative state incorrect? A review of the evidence. *Eur. J. Neurol.* 25 (4), 619–625. <https://doi.org/10.1111/ene.13572>. Epub 2018 Feb 16.
- Zhang, X.-S., Roy, R.J., Jensen, E.W., 2001. EEG complexity as a measure of depth of anesthesia for patients. *IEEE Trans. Biomed. Eng.* 48, 1424–1433.